Remote Sensing of Environment 112 (2008) 3030–3043

Contents lists available at ScienceDirect

Remote Sensing of Environment

journal homepage: www.elsevier.com/locate/rse

PROSPECT-4 and 5: Advances in the leaf optical properties model separating photosynthetic pigments

Jean-Baptiste Feret [a,b,*], Christophe François [b], Gregory P. Asner [c], Anatoly A. Gitelson [d], Roberta E. Martin [c], Luc P.R. Bidel [e], Susan L. Ustin [f], Guerric le Maire [b], Stéphane Jacquemoud [a]

[a] Institut de Physique du Globe de Paris & Université Paris Diderot — Paris 7 (UMR 7154), Géophysique spatiale et planétaire, Case 89, 4 place Jussieu, 75252 Paris Cedex 05, France
[b] Laboratoire Ecologie, Systématique et Evolution (UMR 8079), Université Paris-Sud, 91405 Orsay Cedex, France
[c] Department of Global Ecology, Carnegie Institution of Washington, 260 Panama Street, Stanford, CA 94305, USA
[d] Center for Advanced Land Management Information Technologies, School of Natural Resource Sciences, University of Nebraska-Lincoln, Lincoln, NE 68588-0517, USA
[e] Diversité et Adaptation des Plantes Cultivées (UMR 1097), Laboratoire de Biochimie et Physiologie Végétales, Place Eugène Bataillon, 34095 Montpellier Cedex 05, France
[f] Center for Spatial Technologies and Remote Sensing, Department of Land, Air, and Water Resources, University of California, Davis, CA 95616, USA

ARTICLE INFO

Article history:
Received 20 December 2007
Received in revised form 18 February 2008
Accepted 23 February 2008

Keywords:
Leaf optical properties
Radiative transfer model
PROSPECT
Hyperspectral data
Pigments

ABSTRACT

The PROSPECT leaf optical model has, to date, combined the effects of photosynthetic pigments, but a finer discrimination among the key pigments is important for physiological and ecological applications of remote sensing. Here we present a new calibration and validation of PROSPECT that separates plant pigment contributions to the visible spectrum using several comprehensive datasets containing hundreds of leaves collected in a wide range of ecosystem types. These data include leaf biochemical (chlorophyll *a*, chlorophyll *b*, carotenoids, water, and dry matter) and optical properties (directional–hemispherical reflectance and transmittance measured from 400 nm to 2450 nm). We first provide distinct *in vivo* specific absorption coefficients for each biochemical constituent and determine an average refractive index of the leaf interior. Then we invert the model on independent datasets to check the prediction of the biochemical content of intact leaves. The main result of this study is that the new chlorophyll and carotenoid specific absorption coefficients agree well with available *in vitro* absorption spectra, and that the new refractive index displays interesting spectral features in the visible, in accordance with physical principles. Moreover, we improve the chlorophyll estimation (RMSE = 9 μg/cm^2) and obtain very encouraging results with carotenoids (RMSE = 3 μg/cm^2). Reconstruction of reflectance and transmittance in the 400–2450 nm wavelength domain using PROSPECT is also excellent, with small errors and low to negligible biases. Improvements are particularly noticeable for leaves with low pigment content.

1. Introduction

Improved quantification of vegetation physiology, including the rate of gas exchange with the atmosphere, can be achieved by better measurement and knowledge of the pigments present in plant leaves. There are three types of pigments that determine the leaf color as the result of selective light absorption: chlorophylls (two major types in higher plants, chlorophyll *a* and chlorophyll *b*), carotenoids (including β-carotene and xanthophylls), and anthocyanins. These pigments are present in variable proportions during the differentiation and aging of leaves, but some situations can block their production. For example, the effect of abiotic stress — such as ozone or sulfur dioxide air pollution, heavy metals, viral attack or water deficiency — can cause a change in the optical properties of vegetation. Whereas chlorophyll concentrations can indicate photosynthetic functioning and potential maximum CO_2 assimilation rates, expression of carotenoids can indicate down-regulation of photosynthesis caused by environmental stress. To date, neither of these key pigments groups is well measured from remote sensing data.

The development of precision agriculture has also fueled the need for remote sensing of plant pigments. Since chlorophyll concentration is connected to nitrogen, it has become a key measurement parameter in plant canopies (Gitelson et al., 2003; Ustin et al., 2004, submitted for publication). As for the other foliar pigments, research has concentrated at the leaf scale: carotenes which transfer a fraction of absorbed energy to chlorophylls and which are revealed in leaves in autumn (Gitelson et al., 2002; Merzlyak & Gitelson, 1995); xanthophylls implicated in the photo-regulation of light by dissipating excess

* Corresponding author. Institut de Physique du Globe de Paris & Université Paris Diderot — Paris 7 (UMR 7154), Géophysique spatiale et planétaire, Case 89, 4 place Jussieu, 75252 Paris Cedex 05, France.
E-mail addresses: feret@ipgp.jussieu.fr (J.-B. Feret), christophe.francois@u-psud.fr (C. François), gpa@stanford.edu (G.P. Asner), gitelson@calmit.unl.edu (A.A. Gitelson), remartin@stanford.edu (R.E. Martin), luc.bidel@univ-montp2.fr (L.P.R. Bidel), slustin@ucdavis.edu (S.L. Ustin), guerric.le-maire@cea.fr (G. le Maire), jacquemoud@ipgp.jussieu.fr (S. Jacquemoud).

0034-4257/$ – see front matter © 2008 Elsevier Inc. All rights reserved.
doi:10.1016/j.rse.2008.02.012

absorbed energy, thus avoiding the detrimental oxidation of the photocenter (Gamon & Qiu, 1999); anthocyanins which also protect the photosynthetic system from excess light and whose measurement could indicate the physiological state of plants (Gitelson et al., 2001).

Continuing improvements in the spectral resolution of optical sensors have provided new opportunities for detecting and quantifying individual foliar pigments at large-scales. The radiative transfer models allow an analysis of the remote sensing signal based on robust physical, chemical, and biological processes. PROSPECT (Jacquemoud & Baret, 1990) has become a key model to simulate leaf directional–hemispherical reflectance and transmittance over the whole optical domain (Jacquemoud et al., in press). Several versions of the model have been released since 1990: they correspond to the introduction of new leaf biochemical constituents, mostly cell wall molecules such as cellulose and lignin that compose the dry matter that absorbs shortwave infrared (SWIR) radiation (Baret & Fourty, 1997; Fourty et al., 1996; Jacquemoud et al., 1996, 2000); the spectral resolution was extended from 5 nm to 1 nm by Le Maire et al. (2004) in an unreleased version; and the model was recently adapted to account for leaf surface directional reflectance (Bousquet et al., 2005) and chlorophyll *a* fluorescence emission (Pedrós et al., in preparation). To date, only total chlorophyll, water, and dry matter content are taken into account in the model, and thus retrievable. Pigment discrimination or solar-induced chlorophyll *a* fluorescence measurement using the next generation of hyperspectral sensors requires much finer and more accurate spectral resolutions. The availability of new datasets at 1-nm sampling provides an opportunity to upgrade the model.

In this paper, we first refine the core of PROSPECT by computing a new refractive index spectrum, by setting a more realistic leaf surface roughness parameter, and by developing an optimized calibration process to obtain the relevant specific absorption coefficients for water, dry matter, and the different pigments. Two new versions are developed and compared: PROSPECT-4 and PROSPECT-5, with the latter version providing, for the first time, a physically-based separate treatment of chlorophylls and carotenoids. Inversion methods are then used on independent datasets to validate both models. Biochemical concentration predicted from intact leaves is first compared with measured biochemical composition. Direct comparison between simulated and measured reflectance (and transmittance) is used to assess the performance of the models in terms of accuracy of fit.

2. Need for a new calibration algorithm

PROSPECT simulates the leaf directional–hemispherical reflectance and transmittance (Schaepman-Strub et al., 2006), just named reflectance and transmittance hereafter, from 400 nm to 2500 nm with a minimum number of input variables to facilitate its inversion. The leaf optical properties are mainly driven by the structure parameter N, *i.e.* the number of stacked elementary homogeneous layers, and by the absorption coefficient $k(\lambda)$ of one elementary layer. While optical constants are well known for pure liquid water in the whole electromagnetic spectrum because this molecule received particular attention in physics, chemistry, biology and mineralogy, there are serious gaps in knowledge for plant pigments and cell wall constituents. For that reason, unlike canopy reflectance models, PROSPECT requires a calibration phase where physical and optical constants such as the leaf surface roughness parameter σ, the refractive index of leaf material $n(\lambda)$, and the specific absorption coefficient of leaf absorbers $k_{spe}(\lambda)$ must be determined using experimental data. In the model, these values are assumed to be invariable from one species to another, which is true for $k_{spe}(\lambda)$ but certainly not for σ and $n(\lambda)$ due to the changing nature of leaf surfaces and wax types (Pfündel et al., 2006), and because refraction and absorption are theoretically correlated in a complex medium (Berthier, 1993). In fact, σ and $n(\lambda)$ have not been updated since Jacquemoud and Baret (1990), yet their accuracy is crucial for an improved modeling of leaf optical properties and more accurate retrieval of the biochemical content when inverting the model. PROSPECT is based on physics, consequently it is fundamental to develop a model consistent with our knowledge of these constants (Le Maire et al., 2004).

2.1. Reassessment of the angle of incidence of incoming radiation

When measuring the directional–hemispherical reflectance and transmittance, the incident radiation is perpendicular to the leaf blade that, in fact, intercepts light rays in different directions because its surface is not flat. To mimic the leaf surface roughness on an intuitive basis, the incident radiation in PROSPECT lights up a horizontal plane supposed to be perfectly flat at all angles between 0° (nadir) and 60°. Until now, the value of 60° was empirically set but it seems to be overestimated. In recent work on leaf BRDF modeling, Bousquet et al. (2005) physically linked the probability density function of facet orientations D (Cook & Torrance, 1981) to the surface roughness parameter σ and to the angle α, which is formed by the direction of the leaf normal and the direction of a facet normal:

$$D(\alpha,\sigma)=\frac{1}{\cos^4\alpha}\exp\left(-\left(\frac{\tan\alpha}{\sigma}\right)^2\right). \quad (1)$$

The value of $\sigma \leq 0.5$ was found to be a realistic maximum for most of the leaves. Fig. 1 shows that the actual values of D for $\sigma \leq 0.5$ correspond to an incoming radiation that impinges on the leaf surface at all angles between $\alpha=0°$ and $\alpha=40°$, which appears to be a more realistic value. Moreover, since the average transmissivity at the interface varies very slowly between 0° and 40°, the angle α can be fixed. This allows a slight decrease in the minimum reflectance and an improvement in PROSPECT accuracy at high absorption wavelengths.

2.2. Reassessment of the specific absorption coefficients

The determination of *in vivo* specific absorption coefficients is critical since they link the optical and biochemical properties together. The coefficients of most pigments are actually known *in vitro* for purified molecules dissolved in organic solvents. Because the membrane-bound protein complex is removed during pigment extraction and because spectral shifts may occur in the main absorption peaks, depending on the solvent used to extract them from foliage (Porra, 2002), the *in vitro* specific absorption coefficients cannot be used in PROSPECT. Some *in vivo* absorption spectra can be found in the literature, but they are generally bound to a particular model and expressed in arbitrary units, thus not exploitable.

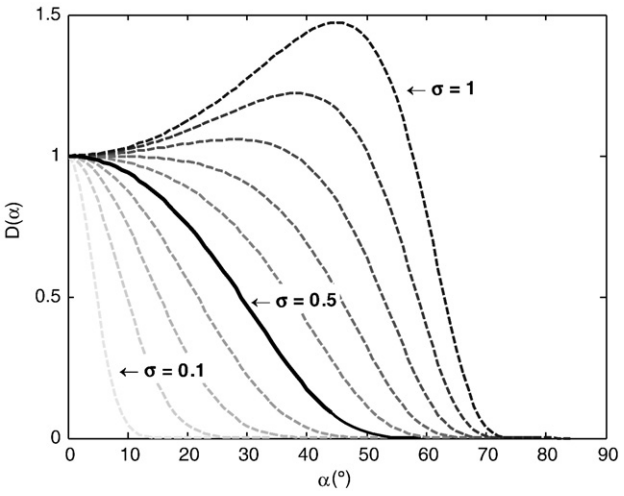

Fig. 1. Adjusted probability density function $D(\alpha)$ of facet orientation α for different values of the roughness parameter σ varying from 0.1 to 1 (after Bousquet, 2007).

Moreover, the overlapping wavelengths of the absorption coefficients of pigments make their identification in leaf reflectance or transmittance spectra difficult to predict. In this context, it is particularly challenging to develop a method to derive the *in vivo* specific absorption coefficients directly from intact leaves *via* spectral measurements and modeling.

2.3. Reassessment of the refractive index

The refractive index $n(\lambda)$ in the previous version of PROSPECT was determined by inversion of the plate model (Allen et al., 1969) using fresh and dry albino maize (*Zea mays* L.) leaves grown under glass. Since then, Le Maire (2005) showed that this continuous smooth spectrum led to inaccuracies in simulated leaf reflectance in the visible (VIS). Thus, both the level and shape of the original spectrum are questionable and should be revised. For instance, $n(\lambda)$ has been assumed to be independent of leaf absorption. The Kramers–Kronig relations however state that the real part of the complex refractive index in a homogeneous medium at a given frequency, subsequently called the refractive index, can be expressed as an integral of the imaginary part, related to absorption, over all frequencies, and vice versa (Berthier, 1993). These relationships are very useful to determine $n(\lambda)$ because it is somewhat difficult to experimentally measure this optical variable over a wide range of frequencies. As an example, Hale and Kerry (1973) successfully computed the refractive index of pure liquid water from its extinction coefficient. Another theory developed by Maxwell Garnett (1904) is required to determine the effective refractive index of an inhomogeneous medium. We however face two kinds of difficulties with plant leaves: first, as pointed out earlier, the absorption properties of the biochemical constituents, except those of water, are poorly known; pigment absorption features are only available *in vitro*, and in most cases only over the VIS. Second, leaves are not homogeneous media. Therefore, a more comprehensive knowledge of absorption and refraction, but also of leaf biochemistry, is required before we can apply a purely theoretical approach to compute $n(\lambda)$ in a complex medium such as a plant leaf. Instead, the refractive index used here was empirically determined without an *a priori* shape constraint.

3. The calibration algorithm

The calibration stage aims at assessing the refractive index $n(\lambda)$ and the specific absorption coefficient $k_{spe}(\lambda)$ of leaf constituents. These are the spectral variables of the plate model that need to be determined wavelength by wavelength. Since leaves cannot be compared to compact layers, the structure parameter N representing leaf anatomy must also be known. N changes from leaf to leaf and is assumed to be wavelength independent, but it cannot be directly measured. Ideally, we should obtain for each leaf the value of N concurrently with the refractive index $n(\lambda)$ and all the $k_{spe}(\lambda)$, which are linearly mixed into the absorption coefficient $k(\lambda)$ of the compact layer. Nevertheless, with spectrophotometric measurements at n_λ wavelengths, such a method would require fitting $2n_\lambda+1$ parameters. The computation of such a large number of unknowns (up to several thousands) is unfeasible. For this reason, the calibration was split in two steps that distinguish between the assessment of N and the assessment of both k_{spe} and n.

3.1. First step: determination of N

Modeling absorption processes first implies that the leaf mesophyll structure is well accounted for by the model. A change in leaf anatomy causes variations in optical properties over the whole spectrum, with a maximum effect in the NIR from 800 nm to 1000 nm where absorption is at a minimum. In fresh leaves, this low absorption is materialized by a plateau of quasi-constant reflectance and transmittance levels at about 40–50% of incident light. This plateau is somewhat disturbed in senescent and dry leaves due to the development of brown pigments or denatured proteins that absorb light below 1300 nm (Baret & Fourty, 1997). We used three wavelengths to perform the inversion and obtain N for each leaf: they correspond to the maximum reflectance (λ_1), the maximum transmittance (λ_2), and the minimum absorptance (λ_3), all three wavelengths located in the NIR plateau (Jacquemoud et al., 1996). The refractive index was set to 1.45 (Woolley, 1975) during this step, but increasing or decreasing it did not fundamentally change the results. Following this procedure, only four variables (leaf structure parameter N together with the three absorption coefficients $k(\lambda_1)$, $k(\lambda_2)$, and $k(\lambda_3)$) were determined for each leaf individually by minimizing the merit function:

$$J(N,k(\lambda_1),k(\lambda_2),k(\lambda_3)) = \sum_{i=1}^{3}\left(R_{mes}(\lambda_i)-R_{mod}(N,k(\lambda_i))\right)^2+\left(T_{mes}(\lambda_i)-T_{mod}(N,k(\lambda_i))\right)^2 \quad (2)$$

where $R_{mes}(\lambda_i)$ and $T_{mes}(\lambda_i)$ are the measured reflectance and transmittance at the wavelength λ_i, and R_{mod} and T_{mod} stand for the modeled values. The optimization is performed using a constrained Powell's line-search method for finding the minimum of the merit function (Press et al., 1992).

3.2. Second step: determination of specific absorption coefficients and refractive index

After the computation of N, the original calibration algorithm of PROSPECT was used to assess the transmission coefficient $\tau(\lambda)$ for each leaf, and afterwards the absorption coefficient $k(\lambda)$ which is directly related to $\tau(\lambda)$ through a Beer–Lambert law integrated over the hemisphere. However, that relationship involving an incomplete gamma function raised numerical problems due to high sensitivity of $k(\lambda)$ to minimal variations of $\tau(\lambda)$. This intermediate step was formerly necessitated by limited computation capabilities. Today, high performance computing capabilities allow direct determination of the specific absorption coefficients by inversion of the model on reflectance and transmittance spectra (Eq. (3)), avoiding these numerical instabilities.

The specific absorption coefficients $k_{spe}(\lambda)$ of leaf absorbers and the refractive index $n(\lambda)$ of leaf material are now computed by inversion of PROSPECT on all leaves comprising the calibration dataset. At each wavelength λ, we minimize the merit function:

$$J(K_{spe,i}(\lambda),n(\lambda)) = \sum_j\left(R_{mes,j}(\lambda)-R_{mod,j}(k(\lambda),n(\lambda))\right)^2+\left(T_{mes,j}(\lambda)-T_{mod,j}(k(\lambda),n(\lambda))\right)^2 \quad (3)$$

where

$$k(\lambda)=\sum_i K_{spe,i}(\lambda)\times\frac{C_i}{N_j}. \quad (4)$$

$k(\lambda)$ is the absorption coefficient of a compact layer at the wavelength λ, C_i the concentration of constituent i, $k_{spe,i}(\lambda)$ the corresponding specific absorption coefficient, and N_j the leaf structure parameter of leaf j. The leaf structure parameters fitted in the first step, as well as the pigment, water, and dry matter contents measured in the laboratory constrain the inversion. The separation of the $k_{spe,i}(\lambda)$ in the inversion process is not straightforward because of overlaps in their main absorption peaks, high correlations between concentrations, and fast saturation of the signal in strong absorption bands. An illustration of the problem is given when assessing the specific absorption coefficient of dry matter, which is hidden by the predominant absorption features of water. This difficulty can be overcome by selecting appropriate datasets containing leaves with a

wide distribution of biochemical concentrations. For pigments, it is particularly important to have light-green or yellowish samples with low concentrations.

4. Available datasets

The previous versions of PROSPECT rely on partial, separate experimental datasets, so that they tend to lack commonness. There is no unique, ideal, perfect experiment dedicated to the calibration of PROSPECT so far. Therefore, we selected four datasets collected by different research teams: the first one called LOPEX dates from 1993 and has been widely used by the remote sensing community (Hosgood et al., 1994); the second one that, for the sake of simplicity, we called CALMIT consists of a subset of 60 fig leaves (*Ficus carica* L.) measured during winter 1995/96 in Israel (CALMIT1, Gitelson et al., 1998a) and a subset of 46 beech leaves (*Fagus Sylvatica*) measured in 1996 in the Black Forest in Germany (CALMIT2, Gitelson et al., 1998b); the third one called ANGERS was measured in 2003 at INRA in Angers (France); and the last one called HAWAII was measured in 2007 in Hawaii (USA) (Asner & Martin, unpublished data). These datasets together encompass hundreds of leaves corresponding to various species, growing conditions (temperate, Mediterranean, and humid tropical), and growth stage. These datasets utilized leaf directional–hemispherical reflectance and transmittance spectra measured in the optical range (<2 nm step) with laboratory spectrophotometers or field spectroradiometers equipped with integrating spheres, and they generally share a pool of biochemical constituents expressed in the same units and are thus comparable: chlorophyll *a* (C_a), chlorophyll *b* (C_b) and total carotenoid (C_{cx}) content, water depth (C_w or EWT for equivalent water thickness), and dry matter content (C_m or LMA for leaf mass per area). In these experiments, leaf discs are generally sampled for biochemicals using a cork borer and extracted immediately after the spectral measurements: their fresh weight was measured before placing them in a drying oven at 85 °C for 48 h and reweighing them to determine the water content (expressed as a percentage), the equivalent water thickness (in cm), and the leaf mass per area (in g/cm^2). At the same time and in the same way, pigments were extracted using organic solvents by grinding fresh or frozen leaf discs in a chilled mortar with a small amount of quartz sand and $MgCO_3$ to prevent acidification. Following centrifugation, the absorbance of the supernatant is measured using dual beam scanning UV–VIS spectrophotometers. Chlorophylls *a*, *b* and total carotenoid content expressed in µg/cm^2 were determined using a multi-wavelength analysis. Table 1 summarizes the main characteristics of these datasets. Notice that this table mentions two different numbers of samples in LOPEX. This dataset contains 580 leaf samples including the optical properties, water and dry matter content for dry and fresh leaves. Five spectral samples were collected for each leaf, and pigment content was integrated into an average whole leaf. 64 fresh leaves were available; each constituent content, reflectance and transmittance spectrum was then averaged over the five samples to obtain the dataset used for the validation of this study.

On the whole, the statistical distribution of pigments, water and dry matter shown in Fig. 2 are consistent within the four datasets, although HAWAII exhibits slightly higher concentrations and LOPEX slightly lower concentrations than the other two datasets. CALMIT1 and CALMIT2, gathered in CALMIT, also show few differences in the pigments repartition: CALMIT2 is similar to ANGERS while CALMIT1 and HAWAII exhibit slightly higher concentrations. The cause of this difference may be due to *i*) datasets collected in different ecosystems, climates, and variety of species. These ecological factors may influence the distribution of pigments in vegetation (Wright et al., 2004). *ii*) A

Table 1
Main characteristics of the datasets

	LOPEX	CALMIT	ANGERS	HAWAII
Date	1993	1996	2003	2007
Number of samples	64/580	106	276	41
Number of species	50	2	49	41
Spectrophotometer/spectroradiometer	Perkin Elmer Lambda 19	Shimadzu UV 2101 PC/LICOR LI-1800	ASD FieldSpec	ASD FieldSpec
Spectral range	400–2500 nm	400–800 nm	400–2450 nm	400–2500 nm
Spectral sampling	1–2 nm (400–1000 nm) 4–5 nm (1000–2500 nm)	1 nm	1.4 nm (350–1050 nm) 2 nm (1000–2500 nm)	1.4 nm (350–1050 nm) 2 nm (1000–2500 nm)
Solvent	Acetone 100%	Acetone 100%	Ethanol 95%	Acetone 100%
Method for pigments	Lichtenthaler (1987)	Lichtenthaler (1987)	Lichtenthaler (1987)	Lichtenthaler and Buschmann (2001)
Chlorophyll a (µg/cm^2)				
Min	0.3	1.0	0.4	13.3
Max	48.0	58.8	76.8	56.3
Mean	15.0	24.2	25.4	37.0
Chlorophyll b (µg/cm^2)				
Min	0.2	0.2	0.3	5.4
Max	14.6	21.1	29.9	21.3
Mean	5	9	8	13
Carotenoids (µg/cm^2)				
Min	0.6	2.0	0	5.1
Max	15.8	18.7	25.3	17.2
Mean	4.4	8.3	8.7	11.8
Water (cm)				
Min	0.0043	n.a.	0.0044	0.0127
Max	0.0439	n.a.	0.0340	0.0713
Mean	0.0113	n.a.	0.0116	0.0275
Dry matter (g/cm^2)				
Min	0.0017	n.a.	0.0017	0.0064
Max	0.0152	n.a.	0.0331	0.0229
Mean	0.0053	n.a.	0.0052	0.0125

In LOPEX, the reflectance and transmittance spectra, as well as the water and dry matter content values, are measured on five different leaves of the same sample, and possibly averaged, while the pigments correspond to a sample of these five leaves.

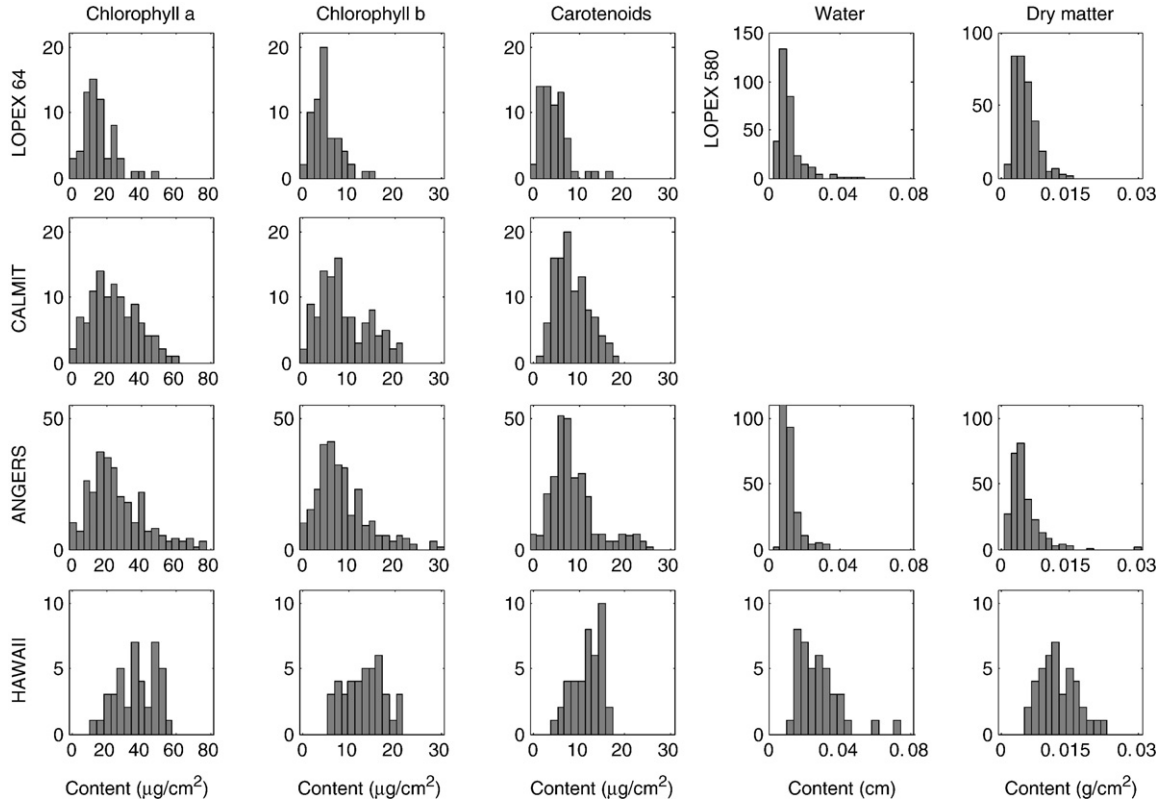

Fig. 2. Distribution of leaf biochemical constituents in the four datasets.

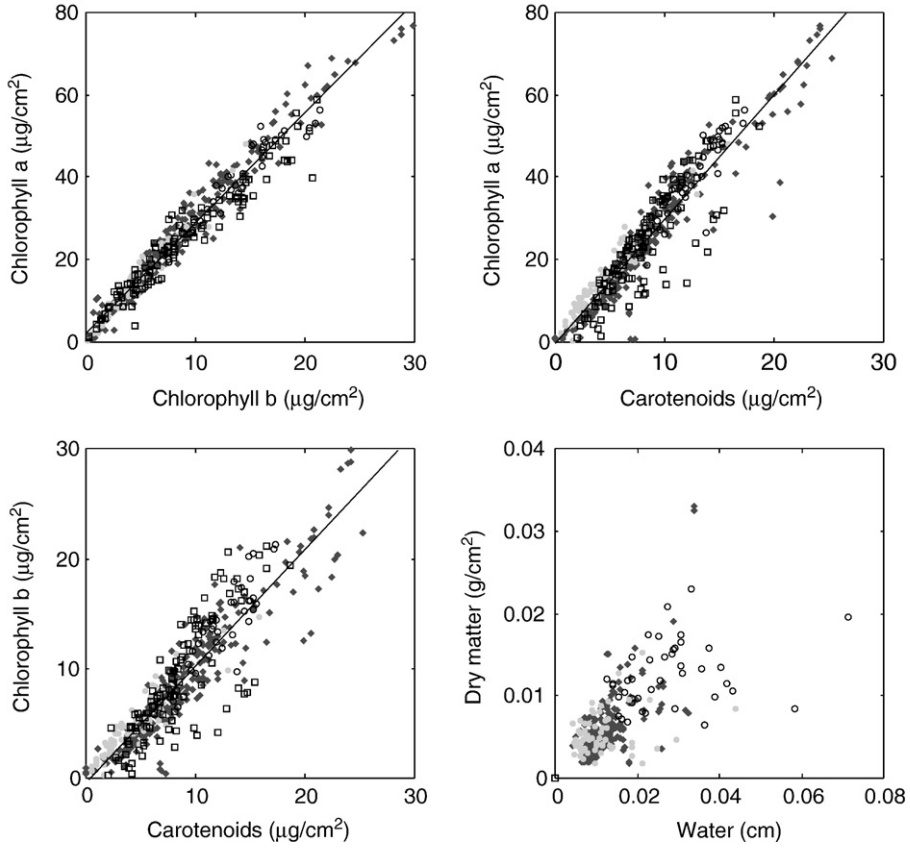

Fig. 3. Pigment, water, and dry matter correlations (● LOPEX □ CALMIT ♦ ANGERS ○ HAWAII).

Table 2
Relationships between pigments in the four datasets, separately and all together

LOPEX	CALMIT	ANGERS	HAWAII	All
$C_a = 3.05C_b +$ 0.46	$C_a = 2.40C_b +$ 3.20	$C_a = 2.78C_b +$ 1.96	$C_a = 2.66C_b +$ 2.07	$C_a = 2.69C_b +$ 2.15
$R^2 = 0.95$	$R^2 = 0.94$	$R^2 = 0.96$	$R^2 = 0.93$	$R^2 = 0.95$
$C_a = 2.99C_{xc} +$ 1.87	$C_a = 3.20C_{xc} -$ 2.51	$C_a = 3.03C_{xc} -$ 0.82	$C_a = 3.49C_{xc} -$ 4.37	$C_a = 3.04C_{xc} +$ 0.44
$R^2 = 0.93$	$R^2 = 0.75$	$R^2 = 0.91$	$R^2 = 0.89$	$R^2 = 0.89$
$C_a = 0.91C_{xc} +$ 0.75	$C_a = 1.20C_{xc} -$ 1.24	$C_a = 1.05C_{xc} -$ 0.66	$C_a = 1.23C_{xc} -$ 1.44	$C_a = 1.07C_{xc} -$ 0.45
$R^2 = 0.85$	$R^2 = 0.65$	$R^2 = 0.88$	$R^2 = 0.83$	$R^2 = 0.83$

different solvent extraction efficiency which may lead to different amounts of pigments extracted from a leaf following the protocol (Porra, 2002).

As expected, strong correlations between concentrations are shown in Fig. 3, which means that they co-vary in nature and that they are not statistically independent. It is particularly interesting to notice that the statistical relationships between C_a, C_b, and C_{xc} are similar in the four datasets (see Table 2). Such relationships appear to be very general, and thus make the separation of pigment effects on spectral optical data challenging to achieve. The gathering of different types of leaves with a wide range of pigments, e.g. obtained by collecting leaves in various physiological states, may help to understand the conditions of stability or variation of these relationships, and to differentiate between individual pigment absorptions.

5. Choice of the datasets used in the calibration

The choice of a dataset suitable for the calibration of PROSPECT is crucial because the coefficients $k_{spe}(\lambda)$ and $n(\lambda)$ largely depend on it. Ideally it should be composed of leaves containing only one absorber in variable amounts. For instance, the absorption of dry matter can be assessed in the NIR and SWIR using dry leaves because absorption, in this spectral domain, is only driven by water and dry matter. LOPEX, which encompasses hundreds of dry leaves, is therefore well adapted. As above-mentioned, it is more difficult to separate leaf photosynthetic pigments because they are strongly correlated and coexist in plants in natural conditions. Albino or etiolated leaves, which would be very useful in this context, are very rare. Calibrations performed using the four available datasets independently were not always consistent, although the leaf constituents are supposed to absorb light the same way. We finally used ANGERS, which is the largest dataset, and the only one to include leaves with very low pigment contents, and sometimes, with almost no carotenoids or no chlorophylls. This distribution results from the sampling strategy: for each plant species, four fully expanded leaves were chosen using nondestructive SPAD measurements in order to have the lowest and the highest possible chlorophyll contents, plus two intermediate values. The availability of spectral endmembers in the calibration dataset is strongly desirable to obtain consistent coefficients. This hypothesis was confirmed when removing leaves with low pigment content from ANGERS during the calibration phase. The degraded leaf variable estimation proved that the model calibration was highly sensitive to such leaves. This result can be easily explained: the presence of pigments quickly increases absorption, tending to hide the contrasts existing between the absorption of each individual constituent. Fig. 4 presents a comprehensive diagram summarizing the structure of the chosen calibration process.

6. Results and discussion

The refractive index and specific absorption coefficients are first determined using LOPEX and ANGERS, and then the performance of the model is assessed on LOPEX, CALMIT, ANGERS, and HAWAII.

6.1. Specific absorption coefficients

6.1.1. Water

Unlike pigments, Jacquemoud et al. (2000) observed that the *in vivo* specific absorption coefficient of water was very similar to that of pure liquid water, thus we decided to use data from the literature

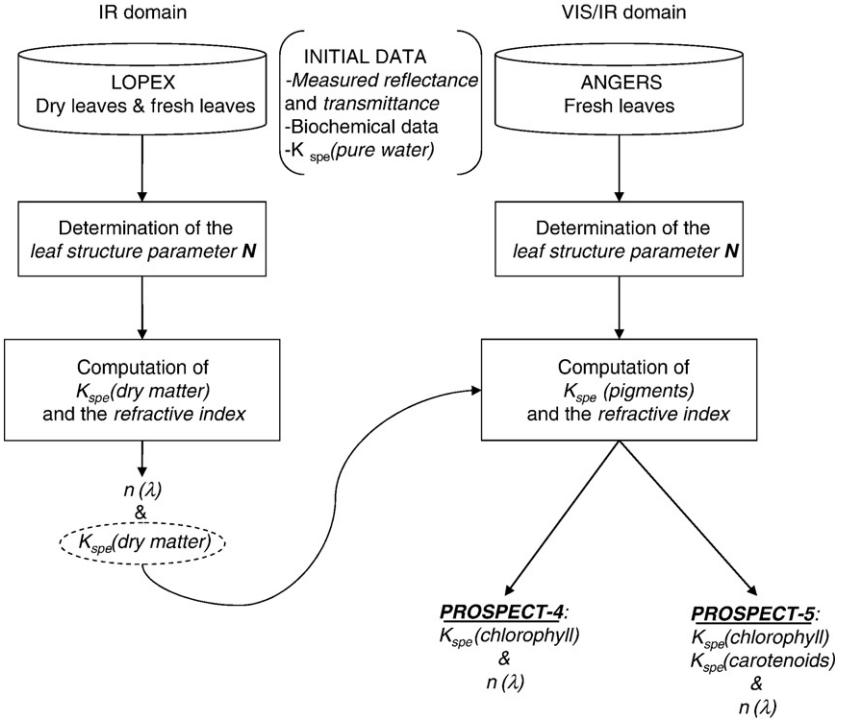

Fig. 4. Diagram of the calibration process.

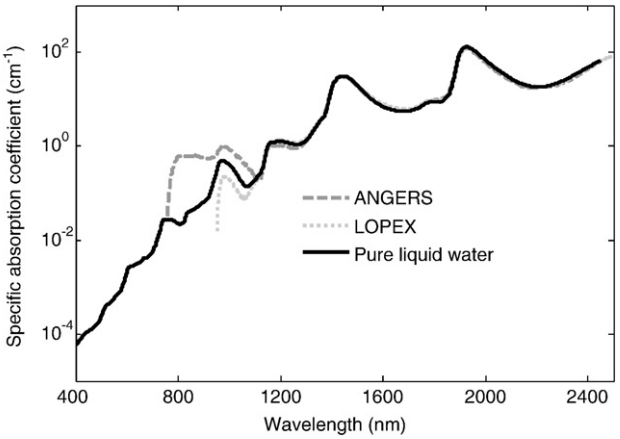

Fig. 5. Specific absorption coefficient of pure liquid water compared to spectra determined with PROSPECT using ANGERS and LOPEX. The specific absorption coefficient of pure liquid water is built from three datasets chosen for their accurate spectral resolution (from 400 nm to 800 nm, Buiteveld et al., 1994; from 800 nm to 1232 nm, Kou et al., 1993; from 1232 nm to 2500 nm, Wieliczka et al., 1989).

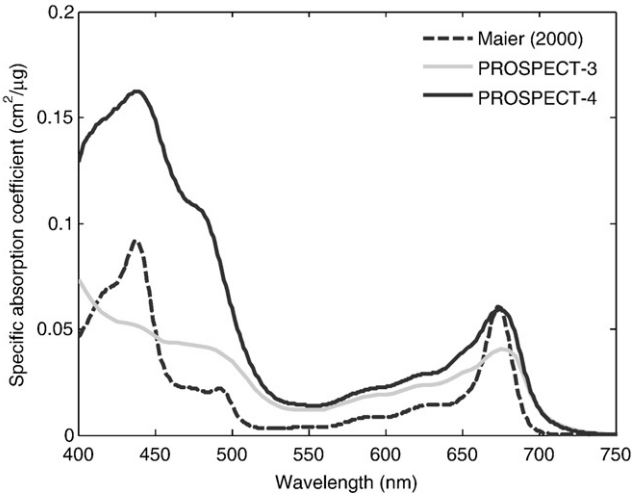

Fig. 7. *In vivo* (PROSPECT-3 and -4) and *in vitro* (after Maier, 2000) chlorophylls *a* and *b* specific absorption coefficient (cm2/µg).

(Buiteveld et al., 1994; Kou et al., 1993; Wieliczka et al., 1989). These data have the advantage of being very accurate in the VIS and the NIR, where, due to very low water absorption and predominance of other absorbers, calibrated coefficients would be senseless. That hypothesis has been validated by re-computing the water specific absorption coefficient, using LOPEX and ANGERS (Fig. 5).

6.1.2. Dry matter

The shape of the estimated specific absorption coefficient spectra for dry matter is not easy to interpret (Fig. 6). In Baret (personal communication), it slowly decreases between 450 nm and 800 nm, while albino leaves (Maas & Dunlap, 1989) clearly show constant absorption in this domain. On the other hand, in Jacquemoud et al. (2000), the high absorption peak below 450 nm, also observed in albino leaves and in leaves with very low pigment content, is absent since their spectrum is constant between 400 nm and 800 nm. The absorption peak in the blue is probably caused by polyphenols (also called phenolic compounds), in particular flavonols (Cerovic et al., 2002). These compounds still exists in fresh foliage, but chlorophylls and carotenoids hide them. However, polyphenols are often correlated with LMA, except for leaves on aging plants (Meyer et al., 2006). From this point forward, we will assume that the stronger absorption between 400 nm and 450 nm is also attributed to dry matter, although it is an approximation.

We selected LOPEX, which contains about 245 dry leaves (placed in a drying oven at 85 °C for 48 h) and 335 fresh leaves, to reassess the specific absorption coefficient of dry matter. From 450 nm to 1200 nm, we set it constant and equal to its minimum value in the IR domain. Fig. 6 presents the spectral variation obtained over the whole optical domain. One can notice that both old and new coefficients are similar in the blue (Baret, personal communication) and IR domains (Jacquemoud et al., 2000).

6.1.3. Pigments

Like former versions, the new model PROSPECT-4 uniformly treats all photosynthetic pigments (chlorophylls and carotenoids), which are assumed to be entirely chlorophyll. The model has been calibrated using the upgraded method and ANGERS. Higher contrasts between non-absorption (550 nm) and absorption wavelengths (450 nm and 680 nm), as well as between these two major peaks, are noticeable in Fig. 7. The new shape, in contrast to the "flatness" of the former version, looks more realistic and is in closer agreement with other estimates from the literature (e.g., Eng & Baranoski, 2007; Maier, 2000). To calculate the *in vitro* specific absorption coefficient of chlorophylls displayed in Fig. 7, we used the Gaussian approximation proposed by Maier (2000) that models the absorption of pigments located in the antenna complexes (LHCP3), assuming a chlorophyll *a*:*b* ratio of about three. One can observe higher values in the 400–500 nm domain that

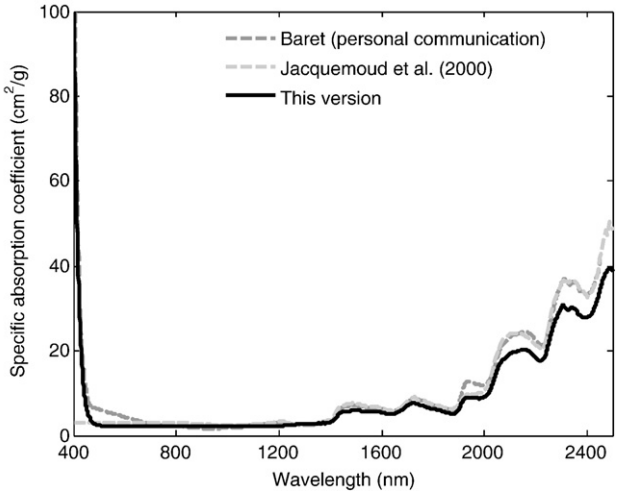

Fig. 6. Specific absorption coefficient of dry matter: former (Baret, personal communication; Jacquemoud et al., 2000) and reassessed.

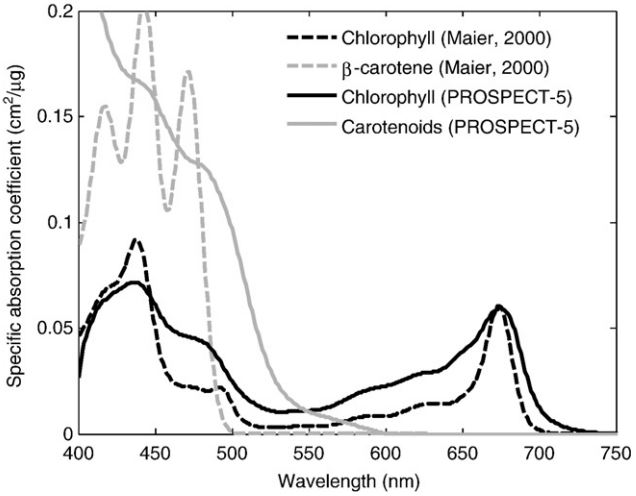

Fig. 8. *In vivo* (PROSPECT-5) and *in vitro* (after Maier, 2000) chlorophyll (black) and total carotenoids (grey) specific absorption coefficients (cm2/µg).

may be explained by additional absorption effects of other pigments, like carotenoids, which are not accounted for in PROSPECT-4.

Another version of the model, PROSPECT-5, was developed to introduce carotenoids in addition to chlorophylls. Results of the corresponding absorption coefficients are presented in Fig. 8.

As expected, differences between the two peaks decrease and get closer to the ratio observed *in vitro*. The chlorophyll absorption peaks at 680 nm are well matched, and the shapes of both curves are in good agreement. The carotenoid specific absorption coefficient also agrees with the literature (Eng & Baranoski, 2007; Maier, 2000). The specific absorption coefficient of carotenoids assessed here integrates the absorption of several pigments (β-carotene, xanthophylls…), by varying their absorption peak. For this reason, no peak is clearly defined when comparing it to the β-carotene proposed by Maier (2000). Note that the modeled carotenoids absorb until 600 nm, while actual carotenoid absorption stops at around 500 nm (Zcheile et al., 1942). The remaining modeled absorption between 500 and 600 nm may be due to the contribution of anthocyanins in low pigment leaves.

Attempts to separate chlorophylls *a* and *b* using the same method unfortunately failed. A classical numerical algorithm fails when variables such as leaf photosynthetic pigments are highly correlated, and this may require further investigations, such as using leaves with unusual pigment combinations, or *a priori* constraints in the merit function. Because the datasets studied in this paper show constant chlorophyll *a*:*b* ratios, separation of these two forms is challenging. This difficulty however should be overcome in the future because of useful applications in chlorophyll fluorescence emission and plant health monitoring (Pedrós et al., in preparation).

6.2. Refractive index

Assuming that the refractive index depends on leaf absorption (see Section 2), each calibration would require the assessment of a new spectrum in accordance with the specific absorption coefficients. For this reason, three different refractive indices have been assessed: one computed using LOPEX simultaneously with the specific absorption coefficient of dry matter, and two computed using ANGERS when calibrating the specific absorption of pigments in both PROSPECT-4 and PROSPECT-5 (Fig. 9). The literature lacks papers providing accurate values of $n(\lambda)$ in the VIS/IR, that would compare to our spectra. Some values averaged in the VIS are available for separate components such as waxes, cellulose, and cell walls (e.g., Brown, 1920; Kumar & Silva, 1973; Woolley, 1975). These authors found that n ranged from 1.41 to 1.55 in fresh leaves, with a mean of 1.45 which fits to our values computed in the VIS with ANGERS. Some differences were pointed out by Woolley (1975) between fresh and dry leaves. One can see in Fig. 9 that the refractive index derived from dry leaves is higher compared to those obtained using fresh leaves or from the previous version. This is in agreement with the measurements on fresh and dry cell walls, which show that the refractive index tends to increase for dry material (Woolley, 1975). Fig. 9 only shows the refractive index of PROSPECT-4 computed using fresh leaves since it is very similar in PROSPECT-5.

The refractive index $n(\lambda)$ calculated using fresh leaves clearly displays unusual spectral features that are probably linked to pigment absorption in the VIS, since they disappear in the refractive index of PROSPECT-3 which has been assessed using an albino maize leaf (Fig. 9). These variations agree with the typical shape of the refractive index obtained by using the Kramers–Kronig relations. It is interesting to note that $n(\lambda)$ obtained from PROSPECT-4 (or PROSPECT-5) is very similar in shape and amplitude to the refractive index of thylakoids (Duniec & Thorne, 1977) or photosynthetic membranes (Paillotin et al., 1998). In this figure, we only present the tangential component of the latter publication, although it originally introduces both the tangential and the normal ones because of the polar coordinate system and spherical symmetry. These two refractive indices mostly differ in their level but not in their shape.

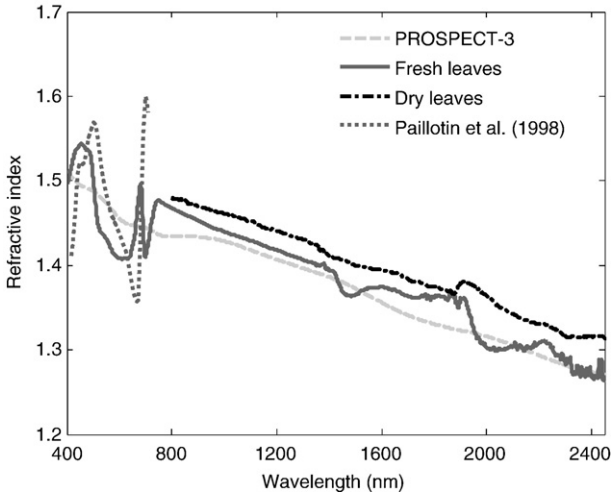

Fig. 9. Refractive index computed from different datasets: based on fresh leaves (ANGERS) and dry leaves (LOPEX) with PROSPECT-4. These refractive indices are compared to the refractive index used in the former version (PROSPECT-3), and the tangential component of the refractive index of the photosynthetic membrane (after Paillotin et al., 1998).

6.3. Performance of the model: biochemical content retrieval

The accuracy of the leaf biochemical constituent retrieval has been assessed through performing a numerical inversion of PROSPECT using reflectance and transmittance spectra. The whole optical domain from 400 nm to 2450 nm has been investigated during the inversion, *i.e.* we determined the water and dry matter content at the same time as leaf pigments. In practice, the inversion consists in finding the parameter set, symbolized by the vector $\boldsymbol{\theta}$, which minimizes the merit function:

$$J(\boldsymbol{\theta}) = \sum_{\lambda_{\min}}^{\lambda_{\max}} \left(R^*(\lambda) - R_{\mathrm{mod}}(\lambda,\boldsymbol{\theta})\right)^2 + \left(T^*(\lambda) - T_{\mathrm{mod}}(\lambda,\boldsymbol{\theta})\right)^2 \quad (5)$$

where R^* and T^* are the measured reflectance and transmittance, and R_{mod} and T_{mod} the modeled ones. Again, the optimization algorithm is a constrained Powell's search method. The accuracy of the prediction and the fit is assessed by the Root Mean Square Error of Prediction (RMSEP), which is equivalent to the Standard Error of Prediction (SEP), the bias (BIAS), and the Standard Error of Prediction Corrected from the bias (SEPC). Let y_j be the measurements, $\bar{y}_j$ their mean, and y_j' the modeled values:

$$\mathrm{RMSEP} = \sqrt{\frac{\sum_{j=1}^{n}\left(y_j' - y_j\right)^2}{n}} \quad (6)$$

$$\mathrm{BIAS} = \frac{\sum_{j=1}^{n}\left(y_j' - y_j\right)}{n} \quad (7)$$

$$\mathrm{SEPC} = \sqrt{\frac{\sum_{j=1}^{n}\left(y_j' - y_j - \mathrm{BIAS}\right)^2}{n}}. \quad (8)$$

The RMSEP is divided into BIAS and SEPC, following the relationship:

$$\mathrm{RMSEP}^2 = \mathrm{SEPC}^2 + \mathrm{BIAS}^2. \quad (9)$$

Since absorption is much more sensitive to variations in small amounts of leaf absorbers, the biochemical constituent retrieval may be more accurate for light-green leaves. The magnitude of the error

Table 3
Validation of pigment, water, and dry matter retrieval using PROSPECT-4 (*P-4*) and PROSPECT-5 (*P-5*)

	LOPEX		CALMIT		ANGERS		HAWAII	
	P-4	*P-5*	*P-4*	*P-5*	*P-4*	*P-5*	*P-4*	*P-5*
Chlorophyll								
– RMSEP (μg/cm^2)	28.92	32.35	7.83	7.06	5.85	5.17	14.25	12.57
– BIAS (μg/cm^2)	26.86	30.07	−2.38	−1.69	−2.32	−1.42	2.48	2.18
– SEPC (μg/cm^2)	10.71	11.91	7.46	6.86	5.37	4.97	14.03	12.38
– CV (%)	54.1	60.1	22.6	20.8	15.8	14.7	28.0	24.7
Carotenoids								
– RMSEP (μg/cm^2)		5.35		3.22		4.22		3.08
– BIAS (μg/cm^2)		2.20		−1.08		−1.95		1.31
– SEPC (μg/cm^2)		4.88		3.03		3.75		2.79
– CV (%)		110.6		36.4		43.3		23.6
Water								
– RMSEP (cm)	0.0017	0.0017			0.0020	0.0020	0.0057	0.0057
– BIAS (cm)	−0.0003	−0.0003	n.a.	n.a.	−0.0001	−0.0001	−0.0015	−0.0015
– SEPC (cm)	0.0017	0.0017	n.a.	n.a.	0.0020	0.0020	0.0055	0.0055
– CV (%)	15.1	15.2	n.a.	n.a.	17.1	17.0	19.8	19.8
Dry matter								
– RMSEP (g/cm^2)	0.0035	0.0034			0.0026	0.0026	0.0049	0.0049
– BIAS (g/cm^2)	0.0021	0.0021	n.a.	n.a.	0.0001	0.0001	−0.0035	−0.0035
– SEPC (g/cm^2)	0.0027	0.0027	n.a.	n.a.	0.0026	0.0026	0.0034	0.0035
– CV (%)	51.1	51.0	n.a.	n.a.	49.8	49.8	27.5	27.8

may consequently be proportional to the constituent content. In this case, Williams (1987) recommends comparing the SEPC with the mean value of the retrieved parameter for evaluating the significance of the error. This index is given by the coefficient of variability (CV) computed as follows:

$$\mathrm{CV} = 100 \times \left(\frac{\mathrm{SEPC}}{\overline{y}_j} \right). \tag{10}$$

The validation of PROSPECT-4 and PROSPECT-5 is presented using the four available datasets. Table 3 summarizes the result of the inversions in terms of RMSEP, BIAS and SEPC obtained for each constituent.

6.3.1. PROSPECT-4

The accuracy of the retrieval varies depending on the leaf constituent. Fig. 10 shows that the estimation of C_w is very good overall. As explained in Section 6.1, water absorption predominates in the IR, so leaf optical properties are mainly influenced by C_w. This also explains the less accurate assessment of C_m. When comparing the performances obtained for each dataset separately, Table 3 shows similar RMSEP (for both water and dry matter retrieval), except in HAWAII, which presents higher water and dry matter contents than the other datasets (Fig. 2). Moreover, when plotting the reflectance and transmittance spectra of leaves issued from HAWAII, very strong absorption is observed in the IR domain. The analysis of the CV shows that the error is proportional to the true value of water content and dry matter content: it is the lowest in HAWAII for the dry matter retrieval, and it is comparable in the three available datasets for water retrieval.

The assessed pigment concentrations are also in good agreement with the measurements, however with a notable exception for LOPEX. Concerning HAWAII, the pigment distribution is higher than in the other datasets, as it is for dry matter and water, which once again may lead to slightly higher RMSEP values. This hypothesis is confirmed by the CV, which is equivalent between HAWAII and CALMIT, and by the results obtained when separating CALMIT1 and CALMIT2: pigment retrieval in CALMIT2 (RMSEP=5.65 μg/cm^2) is much better than in CALMIT1 (RMSEP=9.89 μg/cm^2) because beech leaves contain lower amounts of pigments than fig leaves, and the CV shows that the error is proportional to the true value (CV=25.0% and 21.9%, respectively). As for LOPEX, the chlorophyll retrieval clearly failed (RMSEP>30 μg cm^{-2}), which tends to bring the chlorophyll content of this dataset into question. LOPEX was originally designed to separate the cell wall constituents (lignin, cellulose, etc.) so that emphasis was placed on dry matter and water, while pigment measurements were averaged from five leaf samples. Most of the prediction error for chlorophyll is attributed to a bias. Once corrected for this bias, it is similar to HAWAII

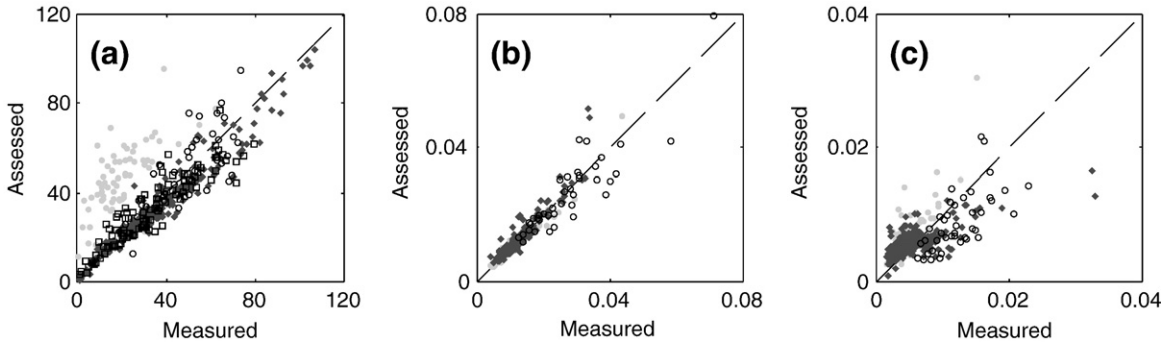

Fig. 10. Comparison between measured and assessed (a) chlorophyll concentration (μg/cm^2), (b) water equivalent thickness (cm), and (c) leaf mass per area (g/cm^2) using PROSPECT-4 (● LOPEX □ CALMIT ♦ ANGERS ○ HAWAII).

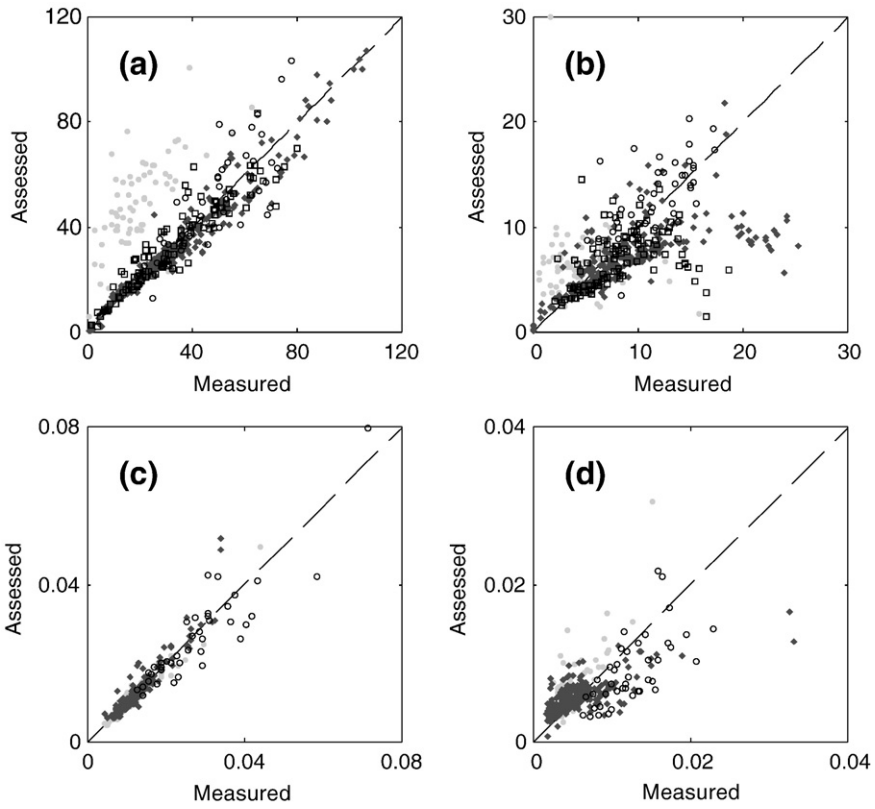

Fig. 11. Comparison between measured and assessed (a) chlorophyll concentration (μg/cm^2), (b) carotenoid concentration (μg/cm^2), (c) water equivalent thickness (cm), and (d) leaf mass per area (g/cm^2) using PROSPECT-5 (● LOPEX □ CALMIT ♦ ANGERS ○ HAWAII).

(see SEPC in Table 3). We believe that the problem originated in the extraction method used to measure the pigments in LOPEX, which may not have been efficient, so that the true pigments content was underestimated compared to the spectral behavior. The lack of accuracy detected with LOPEX does not impact the significance of the calibration of dry matter: the data used for this calibration were available for each leaf, and the weighing was highly reliable.

6.3.2. PROSPECT-5

Water and dry matter retrieval is the same for both versions of PROSPECT that do not differ in the IR. The difference between PROSPECT-4 and PROSPECT-5 is the separation of total chlorophylls and total carotenoids, which improves the chlorophyll retrieval in PROSPECT-5 as shown in Table 3 for ANGERS, CALMIT, and HAWAII (from about 10 μg/cm^2 with PROSPECT-4 to about 9 μg/cm^2 with PROSPECT-5). This slight improvement is due to a better modeling of leaf optical properties, and is particularly significant for light-green leaves. By way of illustration, let us consider sample 254 in ANGERS that has a very low chlorophyll concentration (less than 1 μg/cm^2) and a low C_{ab}:C_{xc} ratio (close to 1). Fig. 12a and b shows that incorporation of carotenoids improves the fit of the model for this sample, whereas there are no noticeable improvements for green leaves (Fig. 12c and d). In this case, whereas PROSPECT-4 offsets the presence of carotenoids by an over-estimation of chlorophyll, PROSPECT-5 manages well to separate the signal of these two pigments. The remaining feature at 700 nm is probably due to the refractive index, which is not appropriate for leaves with low pigment content, as said previously.

The retrieval is less accurate for carotenoids and dry matter than for chlorophyll and water (Fig. 11). These results confirm the expected difficulties due to the strong absorption of chlorophyll and water,

Table 4
RMSEP, BIAS, and SEPC averaged in the VIS (400–800 nm) and IR (800–2450 nm) between measured and simulated reflectance and transmittance for each database, for PROSPECT-4 (*P-4*) and PROSPECT-5 (*P-5*)

	RMSEP		BIAS		SEPC	
	Reflectance	Transmittance	Reflectance	Transmittance	Reflectance	Transmittance
CALMIT						
VIS (*P-4*)	0.039	0.035	0.012	−0.003	0.035	0.031
VIS (*P-5*)	0.032	0.029	0.010	−0.005	0.028	0.025
ANGERS						
VIS (*P-4*)	0.022	0.022	0.002	−0.006	0.022	0.021
VIS (*P-5*)	0.019	0.018	0.001	−0.005	0.019	0.017
IR	0.016	0.016	0.003	0.001	0.014	0.015
HAWAII						
VIS (*P-4*)	0.022	0.021	−0.008	0.002	0.017	0.019
VIS (*P-5*)	0.021	0.022	−0.008	0.003	0.017	0.020
IR	0.036	0.020	−0.031	−0.003	0.017	0.017

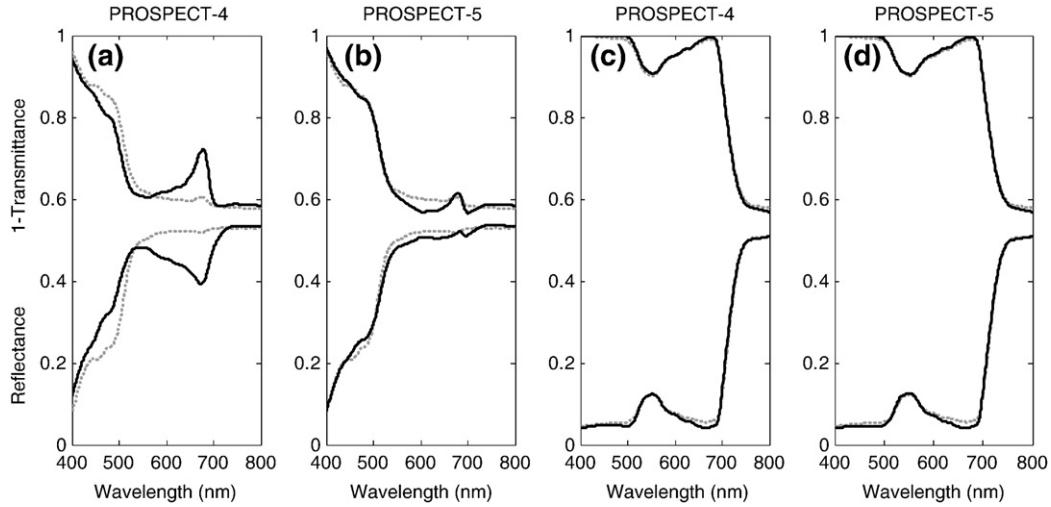

Fig. 12. Comparison of the optical measurement (dotted grey) and the modeling (black) of a low pigment leaf (a and b) and a high pigment leaf (c and d) with PROSPECT-4 and PROSPECT-5.

overshadowing constituents with low absorption power (*i.e.*, dry matter) or low concentration (*i.e.*, pigments other than chlorophyll). However, despite this lower sensitivity, our results show that carotenoids may actually be retrieved from reflectance and transmittance measurements with surprising accuracy (around 3 μg/cm^2).

6.4. Performance of the model

To better appreciate the accuracy of PROSPECT-4 and PROSPECT-5, especially the improvements brought by the upgraded five-variable model, the RMSEP (Fig. 13), BIAS (Fig. 14), and SEPC (Fig. 15) have been calculated for both the reflectance and the transmittance, wavelength by wavelength. For this comparison, we simply used the measured constituents to calculate the leaf reflectance and transmittance. This gives an idea of the performance of the model in direct mode, *i.e.* its ability to represent reality.

6.4.1. Visible domain

The comparison of the RMSEP between PROSPECT-4 and PROSPECT-5 does not show any systematic improvements in the datasets. The modeling of the leaf reflectance and transmittance is clearly better in CALMIT, slightly improved in ANGERS, and no significant variations are observed in HAWAII (Fig. 13 and Table 4). This is due to different pigment distributions (Table 1 and Fig. 2): CALMIT and HAWAII display low and high pigment concentrations, respectively, when a wide range of pigment concentrations has been measured in ANGERS. As seen in Fig. 12, the improvements allowed by PROSPECT-5 are particularly noticeable for low pigment leaves (found in ANGERS

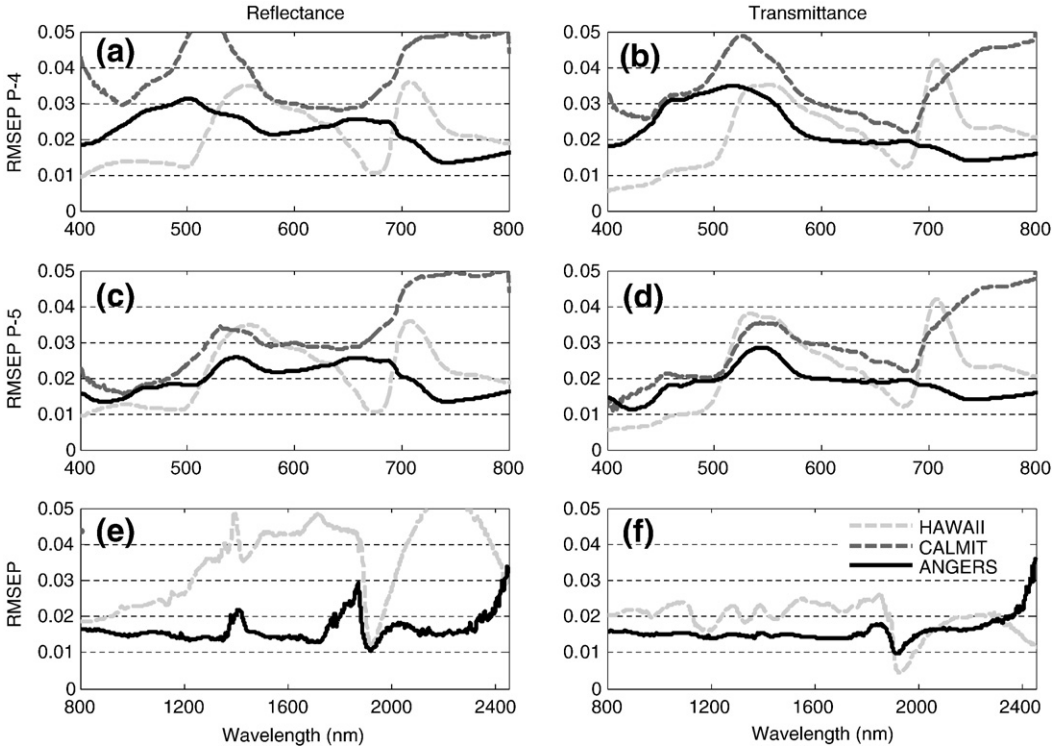

Fig. 13. RMSEP of the modeling of the reflectance and transmittance in the VIS by PROSPECT-4 (a and b), by PROSPECT-5 (c and d) and in the IR by both models (e and f).

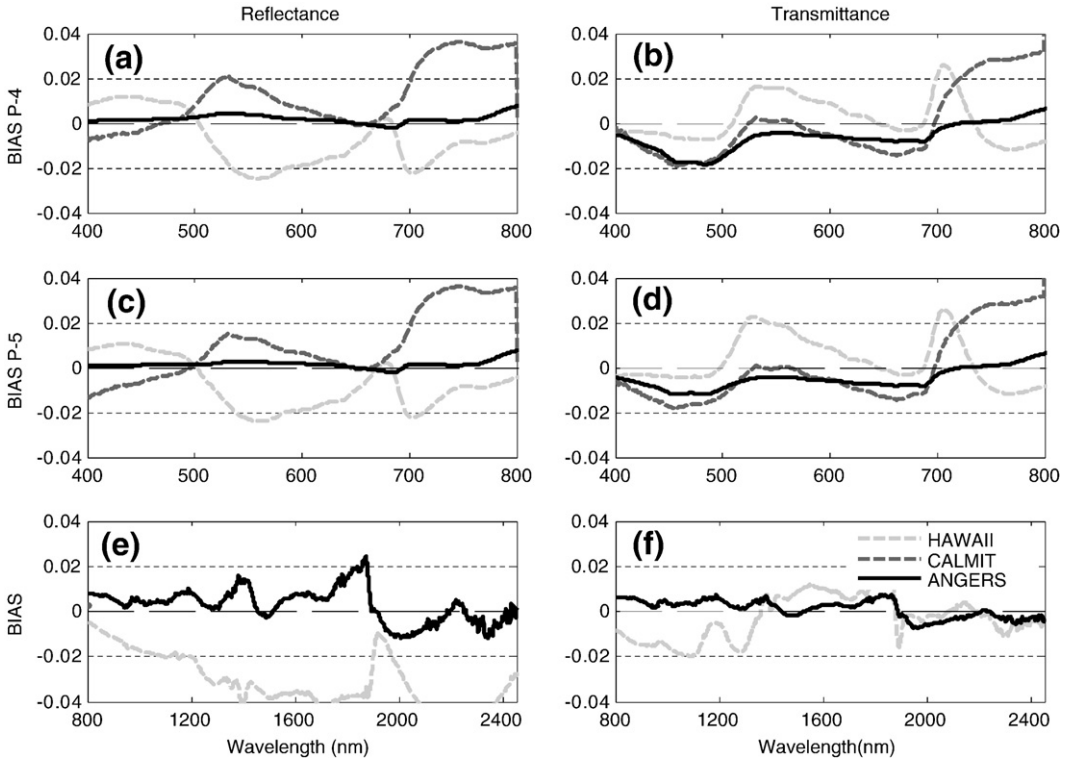

Fig. 14. Bias of the modeling of the reflectance and transmittance in the VIS by PROSPECT-4 (a and b), by PROSPECT-5 (c and d) and in the IR by both models (e and f).

and CALMIT but not in HAWAII) and, to a lesser extent, for high pigment leaves. The least performances when modeling CALMIT beyond 700 nm are due to the missing data for water and dry matter content. The value of these constituent is set to zero, the absorption is only due to chlorophyll, and consequently very underestimated.

6.4.2. IR domain

PROSPECT-4 and PROSPECT-5 are identical in this domain. The difference of RMSEP observed between ANGERS and HAWAII (Fig. 13e) when modeling the reflectance is due to a bias (Fig. 14e), and the SEPC remains mostly lower than 0.02 for both datasets (Fig. 15e).

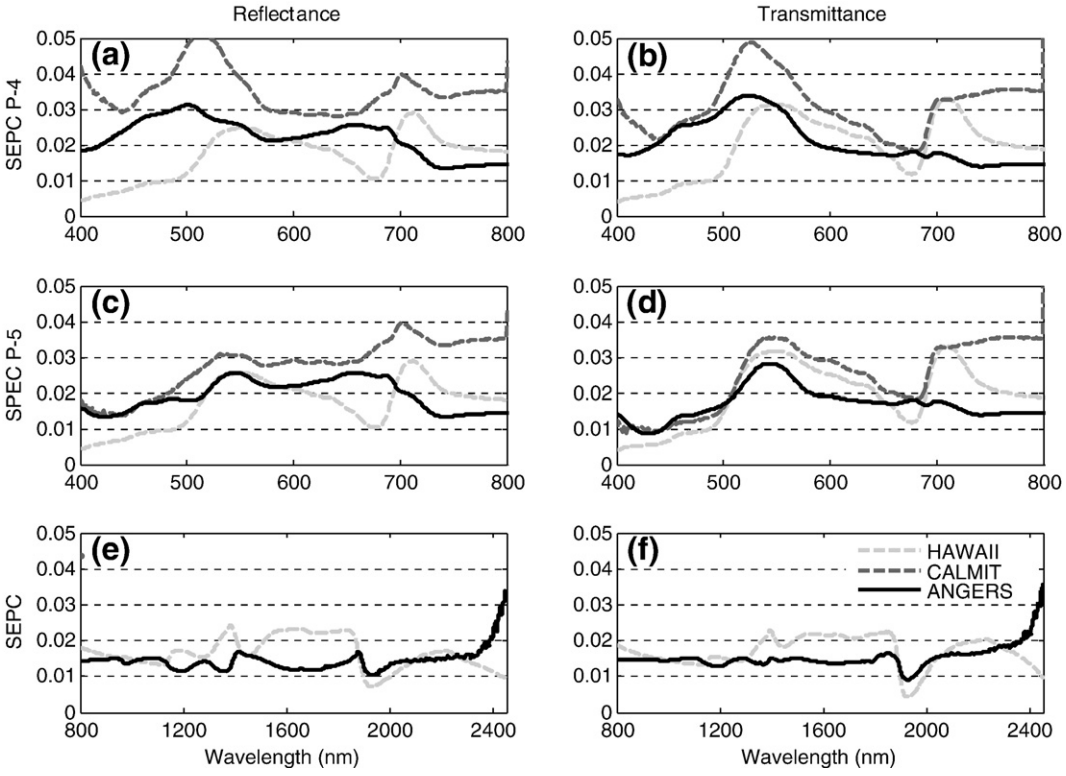

Fig. 15. SEPC of the modeling of the reflectance and transmittance in the VIS by PROSPECT-4 (a and b), by PROSPECT-5 (c and d) and in the IR by both models (e and f).

The performances of PROSPECT-4 and PROSPECT-5 in the direct mode are summarized in Table 4 where all wavelengths have been gathered to obtain a synthetic view of the current state of art in terms of reflectance and transmittance simulations with PROSPECT. The VIS domain includes the 400–600 nm range (where the improvements are noticed), and the 600–800 nm range, which is similar for both versions of the model. The results averaged in the 400–600 nm range show sensibly higher differences between the two versions. Once again, the improvement brought by PROSPECT-5 is observable for both RMSEP and SEPC in CALMIT and ANGERS. To date, the accuracy of PROSPECT in the VIS results in a negligible bias for both reflectance and transmittance, and a RMSEP of about 0.02 to 0.03. Once corrected from the bias, the error in the IR domain is similar in ANGERS and HAWAII.

7. Conclusion

This paper demonstrates that the PROSPECT model, which is currently used as part of the process to obtain biophysical information at the canopy level, can be significantly improved. We succeeded in upgrading the model by optimizing the calibration stage and by using adequate experimental datasets for this purpose (LOPEX for dry matter and ANGERS for pigments). Improved *in vivo* specific absorption coefficients have been determined for each biochemical constituent, as well as a new average refractive index of the leaf interior. *In vivo* chlorophyll and carotenoid-specific absorption coefficients in PROSPECT-5 are in good agreement with *in vitro* absorption spectra. The updated refractive index also displays interesting spectral features in the visible, which agree with the rare experimental data available at present. The main result of this study lies in the improvement of chlorophyll estimation (average RMSEP of 9 $\mu g/cm^2$ with independent datasets) and in very encouraging carotenoid predictions (3 $\mu g/cm^2$). As far as reflectance and transmittance simulations are concerned, the error is around 0.02 to 0.03 and the bias almost nil in the VIS domain, except for transmittance in the IR (around 0.01). When a high accuracy is required between 400 nm and 500 nm, or when the modeling involves light-green leaves, we recommend that the community of researchers use PROSPECT-5.

Besides the addition of carotenoids, our results suggest potential improvements in PROSPECT-5 by including anthocyanins or other pigments involved in the xanthophyll cycle (zeaxanthin, violaxanthin, etc.). The retrieval of carotenoids proved that our method was robust and offered a perspective on the introduction of other absorbing constituents that have a lower influence on leaf optical properties compared to the main ones (because of low contents or low specific absorption coefficients), but that are important in plant physiology. Another avenue of research is on the dependence of the refractive index on pigment concentration. The versions of PROSPECT presented here assume a constant spectrum. Nonetheless, the spectral dependence of the refractive index may be refined in the 400–700 nm range since the Kramers–Kronig relationships link it to the absorption of the leaf. As a result, $n(\lambda)$ would vary from a smooth spectrum for an albino leaf, as in PROSPECT-3, to a shape similar to the one obtained in PROSPECT-4 or -5 but variable with the pigment concentration.

Unlike most former versions, PROSPECT-5 was validated on independent datasets (CALMIT and HAWAII). This work will continue in the frame of a larger project that has just started and that consists in gathering databases containing leaf optical properties together with their biophysical properties. The accuracy of these datasets is crucial to determining correct biochemical contents. We discovered that systematic radiometric or biochemical measurement errors could be detected by model inversion, like pigments in LOPEX.

The efficiency of PROSPECT-5 seems to be established for direct measurements at the leaf level. We encourage the research community to use it and to figure out its validity range, *i.e.* its potentials and limits. Like the previous versions, PROSPECT-5 will shortly be incorporated in the vegetation canopy reflectance model SAIL, to evaluate whether the improvements achieved at the leaf level also apply at the canopy level.

Acknowledgements

We are grateful to the national remote sensing programs for funding this research: INSU Programme National de Télédétection Spatiale (PNTS), CNES Terre Océan Surfaces Continentales Atmosphère (TOSCA) program, NASA Earth Observing System and Terrestrial Ecology programs, the Carnegie Institution of Washington, and the University of California's CalSpace and USDA Hatch programs. IPGP contribution no. 2343.

References

Allen, W. A., Gausman, H. W., Richardson, A. J., & Thomas, J. R. (1969). Interaction of isotropic light with a compact plant leaf. *Journal of the Optical Society of America*, *59*, 1376–1379.

Baret, F., & Fourty, T. (1997). Estimation of leaf water content and specific leaf weight from reflectance and transmittance measurements. *Agronomie*, *17*, 455–464.

Berthier, S. (1993). *Optique des milieux composites.* Polytechnica 300 pp.

Bousquet, L., Lachérade, S., Jacquemoud, S., & Moya, I. (2005). Leaf BRDF measurement and model for specular and diffuse component differentiation. *Remote Sensing of Environment*, *98*, 201–211.

Bousquet, L. (2007), *Mesure et modélisation des propriétés optiques spectrales et directionnelles des feuilles*. Ph.D. Thesis, Université Paris Diderot — Paris 7, Paris (France), 203 pp.

Brown, F. B. H. (1920). The refraction of light in plant tissues. *Bulletin of the Torrey Botanic Club*, *47*, 243–260.

Buiteveld, H., Hakvoort, J. M. H., & Donze, M. (1994). The optical properties of pure water. In J. S. Jaffe (Ed.), *SPIE Proceedings on Ocean Optics XII*, *Vol. 2258*. (pp. 174–183).

Cerovic, Z. G., Ounis, A., Cartelat, A., Latouche, G., Goulas, Y., Meyer, S., et al. (2002). The use of chlorophyll fluorescence excitation spectra for the nondestructive *in situ* assessment of UV-absorbing compounds in leaves. *Plant Cell & Environment*, *25*, 1663–1676.

Cook, R. L., & Torrance, K. E. (1981). A reflectance model for computer graphics. *Computer Graphics*, *15*, 307–316.

Duniec, J. T., & Thorne, S. W. (1977). The relation of light-induced slow absorbancy and scattering changes about 520 nm and structure of chloroplast thylakoids — A theoretical investigation. *Journal of Bioenergetics and Biomembranes*, *9*, 223–235.

Eng, D., & Baranoski, G. V. (2007). The application of photoacoustic absorption spectral data to the modeling of leaf optical properties in the visible range. *Transactions in Geosciences and Remote Sensing*, *45*, 4077–4086.

Fourty, T., Baret, F., Jacquemoud, S., Schmuck, G., & Verdebout, J. (1996). Leaf optical properties with explicit description of its biochemical composition: Direct and inverse problems. *Remote Sensing of Environment*, *56*, 104–117.

Gamon, J. A., & Qiu, H. L. (1999). Ecological applications of remote sensing at multiple scales. In F. I. Pugnaire, & F. Valladares (Eds.), *Handbook of Functional Plant Ecology* (pp. 805–846). New York Marcel Dekker.

Gitelson, A. A., Buschmann, C., & Lichtenthaler, H. K. (1998). Leaf chlorophyll fluorescence corrected from re-absorption by means of absorption and reflectance measurements. *Journal of Plant Physiology*, *152*, 283–296.

Gitelson, A. A., Gritz, Y., & Merzlyak, M. N. (2003). Relationships between leaf chlorophyll content and spectral reflectance and algorithms for non-destructive chlorophyll assessment in higher plant leaves. *Journal of Plant Physiology*, *160*, 271–282.

Gitelson, A. A., Merzlyak, M. N., & Grits, Y. (1998). Remote sensing of chlorophyll concentration in higher plant leaves. *Advances in Space Research*, *22*, 689–692.

Gitelson, A. A., Merzlyak, M. N., & Chivkunova, O. B. (2001). Optical properties and nondestructive estimation of anthocyanin content in plant leaves. *Photochemistry and Photobiology*, *74*, 38–45.

Gitelson, A. A., Zur, Y., Chivkunova, O. B., & Merzlyak, M. N. (2002). Assessing carotenoid content in plant leaves with reflectance spectroscopy. *Photochemistry and Photobiology*, *75*, 272–281.

Hale, G. M., & Kerry, M. R. (1973). Optical constants of water in the 200-nm to 200-μm wavelength region. *Applied Optics*, *12*, 555–562.

Hosgood, B., Jacquemoud, S., Andreoli, G., Verdebout, J., Pedrini, G., & Schmuck, G. (1994). *Leaf Optical Properties EXperiment 93 (LOPEX93).*Ispra (Italy) European Commission — Joint Research Centre EUR 16095 EN, 20 pp. [http://www-gvm.jrc.it/stars/lopex.htm].

Jacquemoud, S., Bacour, C., Poilvé, H., & Frangi, J. P. (2000). Comparison of four radiative transfer models to simulate plant canopies reflectance — Direct and inverse mode. *Remote Sensing of Environment*, *74*, 471–481.

Jacquemoud, S., & Baret, F. (1990). PROSPECT: A model of leaf optical properties spectra. *Remote Sensing of Environment*, *34*, 75–91.

Jacquemoud, S., Ustin, S. L., Verdebout, J., Schmuck, G., Andreoli, G., & Hosgood, B. (1996). Estimating leaf biochemistry using the PROSPECT leaf optical properties model. *Remote Sensing of Environment*, *56*, 194–202.

Jacquemoud, S., Verhoef, W., Baret, F., Bacour, C., Zarco-Tejada, P.J., Asner, et al. (in press), PROSPECT + SAIL models: A review of use for vegetation characterization. *Remote Sensing of Environment*.

Kou, L., Labrie, D., & Chylek, P. (1993). Refractive indices of water and ice in the 0.65- to 2.5-mm spectral range. *Applied Optics*, *32*, 3531–3540.

Kumar, R., & Silva, L. (1973). Light ray tracing through a leaf cross section. *Applied Optics*, *12*, 2950–2954.

Le Maire, G. (2005), Détermination du bilan de carbone de la forêt de Fontainebleau: apports de la télédétection pour la spatialisation des paramètres d'entrée, Ph.D. Thesis, Université Paris Sud, Orsay (France), 200 pp.

Le Maire, G., François, C., & Dufrêne, E. (2004). Towards universal deciduous broad leaf chlorophyll indices using PROSPECT simulated database and hyperspectral reflectance measurements. *Remote Sensing of Environment*, *89*, 1–28.

Lichtenthaler, H. K. (1987). Chlorophylls and carotenoids: Pigments of photosynthetic biomembranes. *Methods in Enzymology*, *148*, 350–382.

Lichtenthaler, H. K., & Buschmann, C. (2001). Chlorophylls and carotenoids: Measurement and characterization by UV–VIS spectroscopy. *Current Protocols in Food Analytical Chemistry* (pp. F4.3.1–F4.3.8). New York John Wiley and Sons.

Maas, S. J., & Dunlap, J. R. (1989). Reflectance, transmittance, and absorptance of light by normal, etiolated, and albino corn leaves. *Agronomy Journal*, *81*, 105–110.

Maier, S.W. (2000), Modeling the radiative transfer in leaves in the 300 nm to 2.5 µm wavelength region taking into consideration chlorophyll fluorescence — The leaf model SLOPE. Ph.D. Thesis, Technische Universität München, Oberpfaffenhofen (Germany), 110 pp.

Maxwell Garnett, J. C. (1904). Colours in metal glasses and in metallic films. *Philosophical Transactions of the Royal Society of London, Series A*, *203*, 385–420.

Merzlyak, M. N., & Gitelson, A. (1995). Why and what for the leaves are yellow in autumn? On the interpretation of optical spectra of senescing leaves (*Acer platanoides* L.). *Journal of Plant Physiology*, *145*, 315–320.

Meyer, S., Cerovic, Z. G., Goulas, Y., Montpied, P., Demotes-Mainard, S., Bidel, L. P. R., et al. (2006). Relationships between optically assessed polyphenols and chlorophyll concentrations, and leaf mass per area ratio in woody plants: A signature of the carbon–nitrogen balance within leaves? *Plant, Cell & Environment*, *29*, 1338–1348.

Paillotin, G., Leibl, W., Gapiński, J., Breton, J., & Dobek, A. (1998). Light gradients in spherical photosynthetic vesicles. *Biophysical Journal*, *75*, 124–133.

Pedrós, R., Goulas, Y., Jacquemoud, S., Louis, J., & Moya, I. (in preparation), FluorMODleaf: A new leaf fluorescence emission model based on the PROSPECT model. *Remote Sensing of Environment*.

Pfündel, E. E., Agati, G., & Cerovic, Z. G. (2006). Optical properties of plant surfaces. In M. Riederer, & C. Müller (Eds.), *Biology of the Plant Cuticle* (pp. 216–249). Blackwell Publishing.

Porra, R. J. (2002). The chequered history of the development and use of simultaneous equations for the accurate determination of chlorophylls *a* and *b*. *Photosynthesis Research*, *73*, 149–156.

Press, W. H., Flannery, B. P., Teukolsky, S. A., & Vetterling, W. T. (1992). *Numerical recipes in FORTRAN: The art of scientific computing.* Cambridge University Press 992 pp.

Schaepman-Strub, G., Schaepman, M. E., Painter, T. H., Dangel, S., & Martonchik, J. V. (2006). Reflectance quantities in optical remote sensing — Definitions and case studies. *Remote Sensing of Environment*, *103*, 27–42.

Ustin, S. L., Asner, G. P., Gamon, J. A., Gitelson, A. A., Huemmrich, K. F., Jacquemoud, S., et al. (submitted for publication), Retrieval of quantitative and qualitative information about plant pigment systems from high resolution spectroscopy, *Remote Sensing of Environment.*

Ustin, S. L., Jacquemoud, S., Zarco-Tejada, P. J., & Asner, G. P. (2004). Remote sensing of the environment: State of the science and new directions. In S. L. Ustin (Ed.), *Manual of Remote Sensing. Volume 4: Remote Sensing for Natural Resource Management and Environmental Monitoring* (pp. 848). John Wiley & Sons.

Wieliczka, D. M., Weng, S., & Querry, M. R. (1989). Wedge shaped cell for highly absorbent liquids: Infrared optical constants of water. *Applied Optics*, *28*, 1714–1719.

Williams, P. C. (1987). Variables affecting near-infrared reflectance spectroscopic analysis. In P. C. Williams, & K. H. Norris (Eds.), *Near-infrared Technology in the Agricultural and Food Industries* (pp. 143–167). St. Paul (MN) American Association of Cereal Chemists.

Woolley, J. T. (1975). Refractive index of soybean leaf cell walls. *Plant Physiology*, *55*, 172–174.

Wright, I. J., Reich, P. B., Westoby, M., Ackerly, D. D., Baruch, Z., Bongers, F., et al. (2004). The worldwide leaf economic spectrum. *Nature*, *428*, 821–827.

Zcheile, F. P., White, J. W., Beadle, B. W., & Roach, J. R. (1942). The preparation and absorption spectra of five pure carotenoid pigments. *Plant Physiology*, *17*, 331–346.